SARS-COV-2 Spike Glycoprotein as Inhibitory Target for Insilico Screening of Natural Compounds

Damilola Alex Omoboyowa (damilola.omoboyowa@aaua.edu.ng)
Adekunle Ajasin University, Akungba-Akoko https://orcid.org/0000-0002-1740-9764

Balogun Toheeb A
Adekunle Ajasin University, Akungba-Akoko

Onyeka S. Chukwudozie
University of Lagos, Nigeria

Victor N. Nweze
University of Nigeria, Nsukka, Nigeria

Oluwatosin A. Saibu
Universitat Duisburg-Essen, NorthRhine-Westphalia, Germany

Alausa Abdulahi
Ladoke Akintola University of Technology, Ogbomoso, Oyo State, Nigeria

Research Article

Keywords: Covid-19, Quercetin-3-o-rutinoside, Spike protein, MD-Simulation

Posted Date: February 23rd, 2021

DOI: https://doi.org/10.21203/rs.3.rs-271483/v1

SARS-COV-2 Spike Glycoprotein as Inhibitory Target for Insilico Screening of Natural Compounds

Damilola A. Omoboyowa[1*], Toheeb A. Balogun[1], Onyeka S. Chukwudozie[2], Victor N. Nweze[3], Oluwatosin A. Saibu[4], Alausa Abdulahi[5]

[1]Department of Biochemistry, Adekunle Ajasin University, Akungba-Akoko, Ondo State, Nigeria

[2]Department of Cell Biology and Genetics, University of Lagos, Nigeria

[3]Department of Biochemistry, University of Nigeria, Nsukka, Nigeria

[4]Department of Environmental Toxicology, Universitat Duisburg-Essen, NorthRhine-Westphalia, Germany

Department of Biochemistry, Ladoke Akintola University of Technology, Ogbomoso, Oyo State, Nigeria

Abstract

Coronavirus disease 2019 (Covid-19) pandemic caused by SARS-Cov-2 has raised global health concern without approved drug for management of this lie threatening disease. The aim of this study was to predict the inhibitory potential of quercetin-3-o-rutinoside against SARS-Cov-2 spike glycoprotein. Targeting the SARS-Cov-2 spike protein from angiotensin converting enzyme 2 complex (pdb: 6lzg) is gaining importance. In this study, *in silico* computational relationship between plant-derived natural drug and spike glycoprotein was predicted. The results were evaluated based on glide (Schrodinger) dock score. Among the five (5) screened compounds, quercetin-3-o-rutinoside has the best docking score (-9.296) with the target. Molecular dynamic (MD) simulation study was performed for 1000ps to confirm the stability behavior of the spike protein and quercetin-3-o-rutinoside complex. The MD simulation study validated the stability of quercetin-3-o-rutinoside in the spike protein binding pocket as potent inhibitor.

Keywords: Covid-19; Quercetin-3-o-rutinoside; Spike protein; MD-Simulation

Introduction

Coronavirus (Cov) belongs to the family coronaviridae, considered to be the largest RNA virus with genomes ranging from 27 to 32kb (Masters, 2016; Rahman et al., 2020). Coronavirus disease 2019 (Covid-19) is a major life threatening disease worldwide due to its fast spreading (Kadioglul et al., 2020). It is caused by severe acute respiratory syndrome coronavirus 2 (SARS-Cov-2) (Omotuyi et al., 2020). The SARS-Cov-2 causes mainly severe acute and other complications in the heart, kidney, brain and spleen ultimately leading to disastrous effect in

Covid-19 afflicted patients (Madjid et al., 2020). SARS-Cov-2 invade human cells through its spike proteins interaction with angiotensin converting enzyme 2 (ACE 2) receptors. As a structural glycoprotein on the virion surface, the spike glycoprotein of coronavirus binds to the host cellular receptors followed by fusion between the viral envelope and the cellular membrane (Zhang et al., 2005). Upon binding with the receptor, the protein changes its conformation from a pre-fusion to a post-fusion form (Pandey et al., 2020).

The viral glycosylated spike protein composed of S1 and S2 subunits in the coronavirus which enables them access into the host cell. The receptor bonding domain of S1 subunit in SARS-CoV-2 attaches to ACE2, led to the shed of S1 subunit and subsequently triggers the cleavage of the S2 subunit by the host protease protein (Hoffman et al., 2020). The biophysical and structural evidence shows that, SARS-CoV-2 spike protein binds with ACE2 receptors with higher affinity (Patel et al., 2020). Therefore, it is a target for small molecules to generate potential inhibitors of ACE2 interaction with the protein.

In silico studies of small molecules including those of natural compounds of plant origin have been screened and confirm to directly inhibit this important protein of SARS-Cov-2 (Zhang et al., 2020; Chen et al., 2020; Wen et al., 2007). Although drug development against coronavirus (Covid-19) has poses great challenge to scientist. However, the virtual screening of databases and the use of bioinformatics and cheminformatics have improved the discovery of small molecules that binds to the selected target which is the preliminary phase of drug design. Here, five natural compounds were screened, targeting the entry pathway of SARS-Cov-2 penetration into cells. The Quercetin and Kaempferol derivatives screened in this study are widely distributed plant flavonoids, found in several vegetables, seeds, grains (Biancatelli et al., 2020) and other plant parts. Studies suggested that these compounds promote antioxidant (Robazkiewics et al., 2007), anti-inflammatory (Nair et al., 2002), antiviral and immune-protective potentials (Uchide and Toyoda, 2011).

Quercetin has been studied in various models of viral infection due to its antiviral efficacy through inhibition of protease, ploymerases, DNA gyrase suppression and reverse transcriptase inhibition (Biancatelli et al., 2020).

In this *in silico* study, molecular docking and molecular dynamics simulation were performed to ascertain the most potent inhibitory compounds against SARS-CoV-2 spike protein. The

pharmacokinetics properties of these natural compounds were also explored to ascertain these compounds as therapeutic agents.

METHODOLOGY

Materials and method

Glide tool from Schrodinger molecular drug discovery suite (version 2017-1) and AMBER 16 package were used for molecular docking and MD simulation respectively in this research.

Ligand Preparation

Five (5) phyto-compounds of rutin derivatives used in this research were obtained from published literatures and they were used to prepare the library for this research. The structures of the phytochemicals were downloaded in the Structure data format (sdf format) from the PubChem database (https://pubchem.ncbi.nlm.nih.gov). The ligands were prepared by LigPrep module of Maestro 11.5 interfaces in the Schrodinger suite 2017-1. They were converted from 2D to 3D structures by including stereo chemical, ionization, tautomeric variations, as well as energy minimization and optimized for their geometry, desalted and corrected for their chiralities and missing hydrogen atoms. The bonds orders of these ligands were fixed and the charged groups were neutralized. The ionization and tautomeric states were generated between pH of 7.0 +_ 2.0 using Epik module. In the LigPrep module, the compounds were minimized by Optimized Potentials for Liquid Simulations (OPLS3) force field. A single low energy ring confirmation per ligand was generated and the optimized ligands were used for docking analysis (Balogun et al., 2020).

Protein Preparation

Nucleocapsid spike glycoprotein crystal structure of SARS-CoV-2 was retrieved from Protein Data Bank (http://www.rcsb.org/pdb/home.do) (pdb ID: 6M3M). The maestro11.5 interface was used to view the 3D structure of SARS-CoV-2 nucleocapsid spike glycoprotein. The protein was prepared according to Balogun *et al.* (2020).

Nucleocapsid spike glycoprotein grid Generation

Using the module for generating receptor grid on maestro 11.5, the area of interaction between the nucleocapsid spike glycoprotein and ligands were generated. The centroid of the docked pose, in the binding box dimension of the spike protein, was patterned in terms of the coordinates x, y and z.

Molecular docking using glide tool

Using the prepared spike glycoprotein and ligands, the molecular docking of the molecules was carried out on maestro11.5 from Schrödinger 2017-1. The phytochemicals of P. dulcis were docked into the active site of the protein according to extra precision mode (X-P) alongside sampling of the ligands as none refine only. The ligand interaction tool was used to view the ligand interaction with the amino acid residues at the binding pocket of the protein (Balogun *et al.,* 2020).

Pharmacokinetics screening of hit Compounds

The ADME toxicity depicts the absorption, distribution, metabolism, excretion, toxicity, and elucidates the pharmacokinetics profiles of the natural compounds. The ADME toxicity screening of the natural compounds were performed with the admetSAR prediction online tool (http://lmmd.ecust.edu.cn:8000/) (Cheng et al., 2012).

Molecular Dynamics Simulations

The molecular dynamics simulation was conducted at a simulation time of 10000 ps using the AMBER 16 package. The topology files of the superimposed complex were constructed using the in house program of the package. The antechamber program was used to assemble the force fields for the receptor residues and ligand molecules, while for the construction of the biopolymers from the component residues and preparation of the force field, the LEaP plugin was used. The AMBER ff14SB (Maier et al., 2015) and gaff force field (Wang *et al*., 2004) were used for the receptor amino residue and the ligand complex. The electrostatic interactions are handled by a particle-mesh Ewald (PME) protocol, and long-range Lennard–Jones attractions are

treated by a continuum model. This gives densities and cohesive energies of simple liquids that are in excellent agreement with more elaborate methods (Horn et al. 2004).The distribution of the viral receptors and the compounds RSMD were displayed with histogram using R package, and the associated hydrogen bonding receptor and hydrogen bonding acceptor between the ligands and viral receptors at each picoseconds were calculated. Using one of the program plugins such as the MDTraj (McGibbon et al. 2015), the nonnative contact was calculated, and using the Bio3d the residue cross correlation was calculated (Grant et al. 2006).For the trajectory analysis, parameters considered were radius of Gyration (Rg), Root Mean Square Devaitaion (RMSD), Fraction of Native Contacts (Q), Root Mean Square Fluctuation (RMSF), B-factor, Principal Component Analysis (PCA), dynamic cross-correlations analysis, hydrogen bond analysis, and energy calculations.

RESULTS AND DISCUSSION

Molecular docking Result

The molecular docking analysis was performed for the prediction of potential compounds which can inhibit the SARS-Cov-2 spike protein. Although, all the screened compounds exhibited good docking score (figure 1), literature search showed that quercetin had history as antioxidant, anti-inflammatory and anti-viral potential (Biancatelli et al., 2020), therefore, selected for further computational investigation. The choice of quercetin-3-o-rutinoside was further supported by the findings of Heinz et al., (2010) who reported quercetin supplementation and upper respiratory tract infection in a randomized community clinical trial. The selective inhibition of quercetin-3-o-rutinoside towards SARS-CoV-2 spike protein is probably due to the formation of six hydrogen bond interactions with spike glycoprotein (ALA-139, TRY-133, ARG-69, LYS-66 and GLY-126 (Fig. 2).

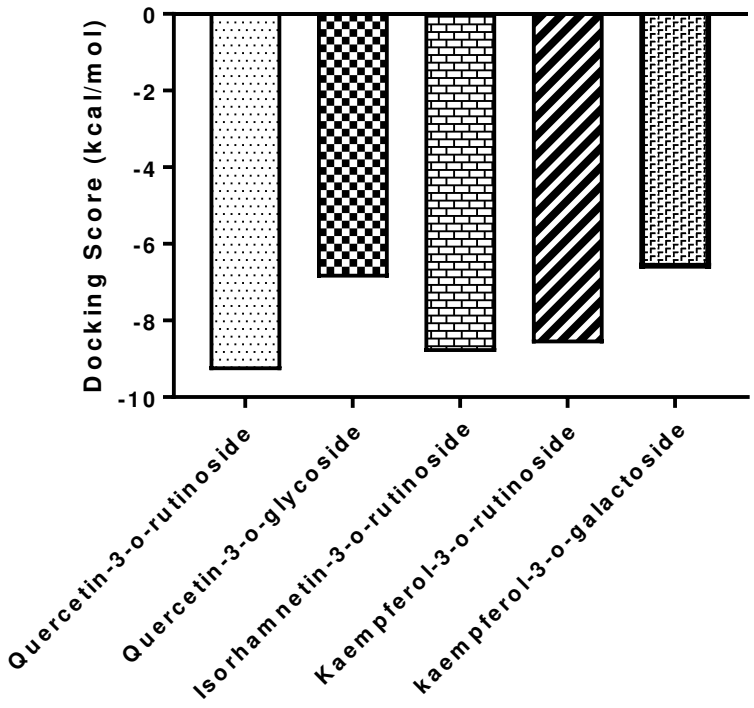

Fig. 1: The binding affinity (kcal/mol) for the docking of the natural compounds against Nucleocapsid Spike Glycoprotein

Table 1: Docking Results of Natural Compounds against Nucleocapsid Spike Glycoprotein

S/N	Entry Name	Dock score	Glide score	Glide model
1.	quercetin-3-o-rutinoside	-9.296	-9.308	-74.457
2.	isorhamnetin-3-o-rutinoside	-8.823	-8.834	-71.423
3.	kaempferol-3-o-rutinoside	-8.598	-8.610	-77.458
4.	quercetin-3-o-glucoside	-6.877	-6.888	0.000
5.	kaempferol-3-o-galactoside	-6.648	-6.660	-56.932

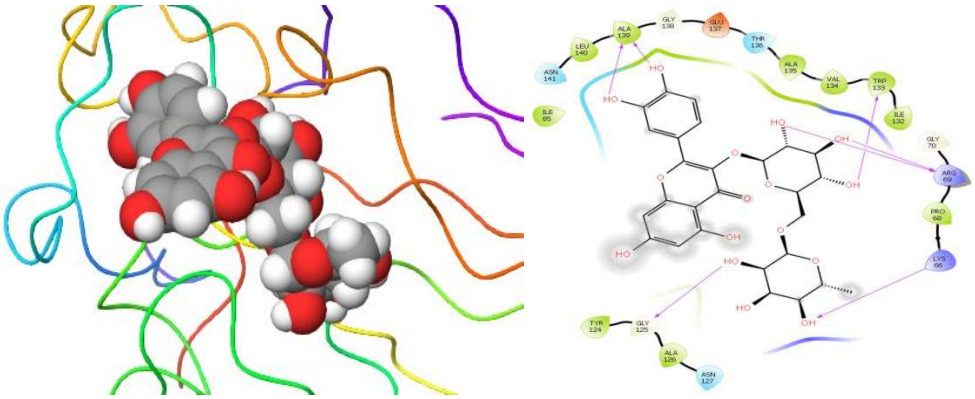

Fig. 2: Protein-ligand interaction of quercetin-3-o-rutinoside against spike glycoprotein

Pharmacokinetics profile of the natural compounds

In silico ADMET screening technique has proved reliable in prediction of pharmacokinetics profile of therapeutic agents (Verbe et al., 2002). Most readily available drugs are administered through the oral route for the efficacy of such drugs; it must be absorbed into the bloodstream (Yan et al., 2008). Table 2 showed that all the natural compounds are human intestinal absorption (HIA) positive; these compounds can be absorbed into the bloodstream for systemic circulation. The failure of most promising drugs is the presence of barriers between blood and brain (Ballabh et al., 2004). All the compounds under investigation cannot cross the barrier between blood and brain (BBB-). Therefore, administration of these compounds cannot result into neurological disorders. The p-glycoprotein (p-gp) is an efflux membrane transported. It hinders the retention, permeability and absorption of drugs that are its substrates channeling them out of the cells. Table 2 showed that, all the compounds are non-substrate of p-glycoprotein, hence, thrusting them out of the cell. The evaluation of therapeutic agents relies on its ability to inhibit or act as substrate for CYP_{450} isoforms which help to predict the disposition, efficacy or toxicity of synergistic administration with known CYP_{450} substrate (Zhou et al., 2008). From table 2, all the natural compounds are non-substrate and non-inhibitor of CYP_{450} 2C9, 2D6, 3A4 and 1A2 except kaempferol-3-o-rutinoside which was observed as substrate of CYP_{450} 3A4. Therefore, co-administration of other drugs does not posse drug-drug interaction or toxicity. From table 2, all the natural compounds are non-carcinogenic and non-toxic compounds.

Table 2: Pharmacokinetics profile of compounds

Profile	quercetin-3-o-rutinoside	quercetin-3-o-glucoside	isorhamnetin-3-o-rutinoside	kaempferol-3-o-rutinoside	kaempferol-3-o-galactoside
Absorption					
BBB	-	-	-	-	-
HIA	+	+	+	+	+
$CaCO_2$ P.	-	-	-	-	-
P-gp inhibitor	Non substrate Non-inhibitor	Non substrate Non-inhibitor	Non substrate Non-inhibitor	Non substrate Non-inhibitor	Non substrate Non-inhibitor
Distribution					
Subcellular localization	Mitochondria	Mitochondria	Mitochondria	Mitochondria	Mitochondria
Metabolism					
CYP_{450} 2C9 substate/inhibitor	Non substrate Non inhibitor	Non substrate Non inhibitor	Non substrate Non inhibitor	Non substrate Non inhibitor	Non substrate Non inhibitor
CYP_{450} 2D6 substate/inhibitor	Non substrate Non inhibitor	Non substrate Non inhibitor	Non substrate Non inhibitor	Non substrate Non inhibitor	Non substrate Non inhibitor
CYP_{450} 3A4 substate/inhibitor	Non substrate Non inhibitor	Non substrate Non inhibitor	Non substrate Non inhibitor	Substrate Non inhibitor	Non substrate Non inhibitor
CYP_{450} 1A2 inhibitor	Non inhibitor	Non inhibitor	Non inhibitor	Non inhibitor	Non inhibitor
Toxicity					
AMES toxicity	Non AMES toxic	AMES toxic	Non AMES toxic	Non AMES toxic	Non AMES toxic
Carcinogens	Non-carcinogen	Non-carcinogen	Non-carcinogen	Non-carcinogen	Non-carcinogen
Acute oral toxicity	III	III	III	III	III

Note: BBB: Blood Brain Barrier; HIA: Human Intestinal Absorption; $CaCO_2$ P.: $CaCO_2$ Permeability; p-gp: P-glycoprotein; CYP_{450}: Cytochrome P_{450}

Molecular Dynamics of protein-ligand complex

The molecular analysis lead to the selection of quercetin-3-o-rutinoside which showed best inhibitory activity against SARS-Cov-2 spike protein. Biological activities may result in comformational changes in protein structure, also aqueous environment sorrounding protein plays major role in the interaction of protein-ligand complex (Pandey et al., 2020). Hence, molecular dynamics simulation in solvated environment was performed to investigate the conformational stability of quercetin-3-o-rutinoside binding to the active site of SARS-CoV-2 spike protein.

The RSMD for the spike protein was 2.5 Å, at a simulation time of 1ns, signifying the stability of the protein during the course of the simulation. At the same simulation time of 1ns, the RSMD of the ligand was 3.0 Å (Figure 3a and 3b).

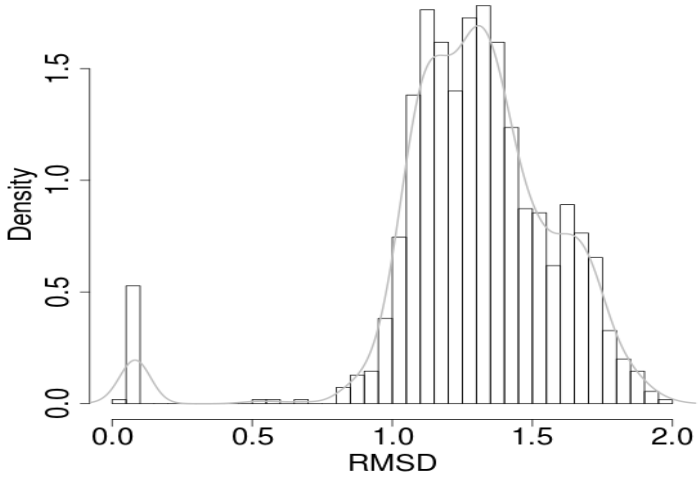

Fig 3a: Generated RSMD histogram of the spike receptor

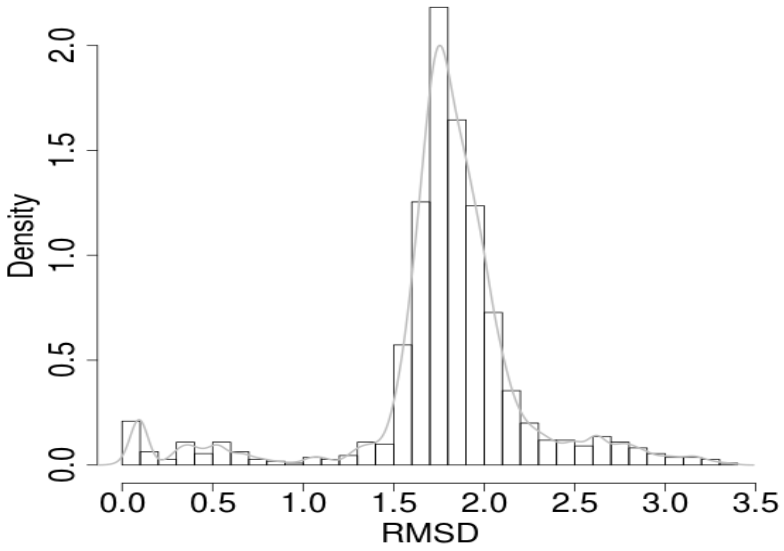

Fig 3b**:** Generated RSMD plot for the ligand

Given the docked complex between quercetin-3-o-rutinoside and SARS-CoV-2 spike protein, moelcular dynamics (MD) simulations provides detials about the atomic movements characterizing the interaction. With this, the stereochemical behaviour of the docked complex is assessed. The Generated Root Mean Square Devaitaion (RMSD) plot indicates equilibrum or stability between the superimposed complex, which depends on the binding interaction and energy between the spike receptor and ligand.

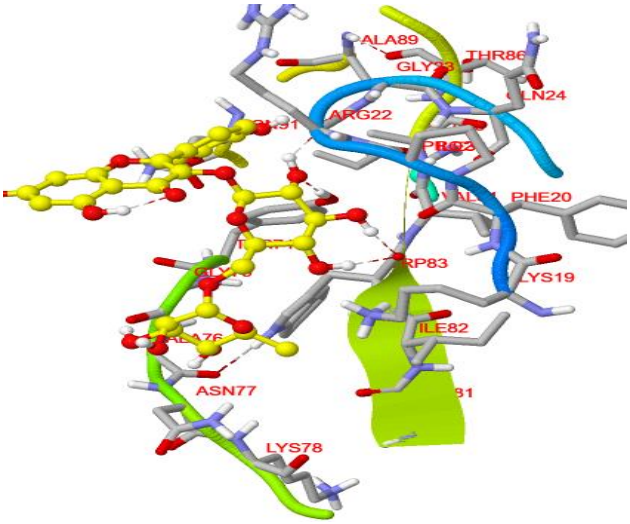

Fig. 4: Native contacts between Spike protein residues and quercetin-3-o-rutinoside complex.

Assessing the native contacts between the protein and quercetin-3-o-rutinoside, there were variations in the number of hydrogen residual bonds interacting with the quercetin-3-o-rutinoside at different simulation time scale (Figure 4). At the final simulation time of 1000 ps, four (4) hydrogen atom were obsered interacting with quercetin-3-o-rutinoside (Figure 5a). The RSMD crystallography resolution of the docked complex, ranged from 1.5 to 2.9Å at a simulation time of 1000ps, which signifies that both relationship are linear (Fig 5b). A resolution outside this range, denotes that the complex can't be linear. The protein had a conformational change as indicated by the RSMD. The start of the ligand RSMD fluctuation was observed at a simulation time of 800 ps, which therefore continues till the end of the simulations. This is an indication that quercetin-3-o-rutinoside form unstable binding pose with the binding pocket of the protein target. The protein residue fluctuations after continous linear attribute, was observed at 600 ps, and at around the simulation time of 800 ps, stability was sustianed throughout the simulation period. In summary, the ligand was relatively stable, which implies that it form stable bound with the spike protein and have not diffused away from the binding pocket of the protein.

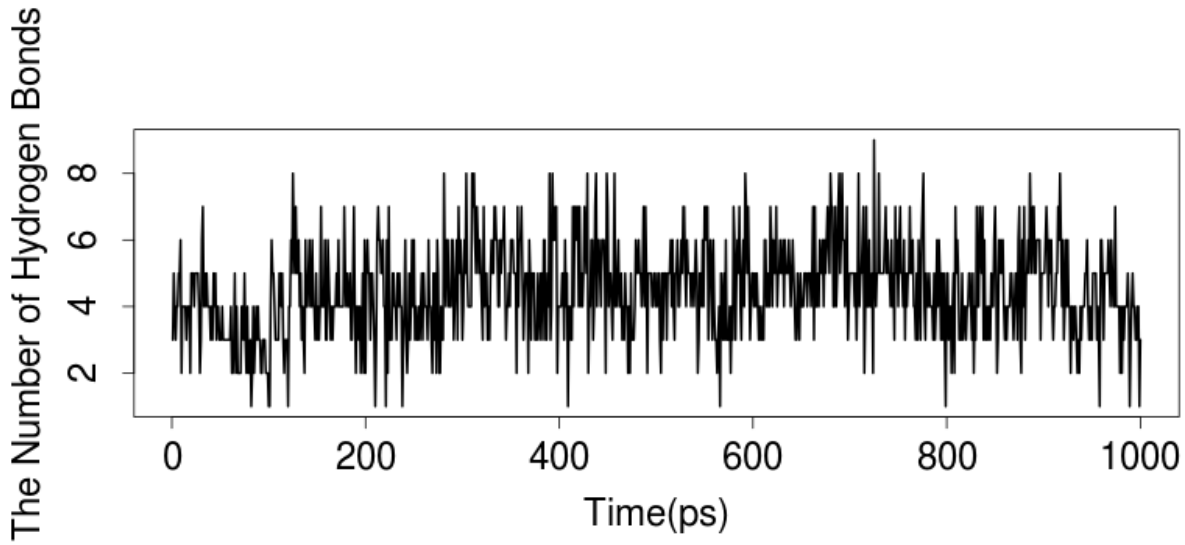

Fig. 5a: The number of hydrogen interactions between the ligand and the protein.

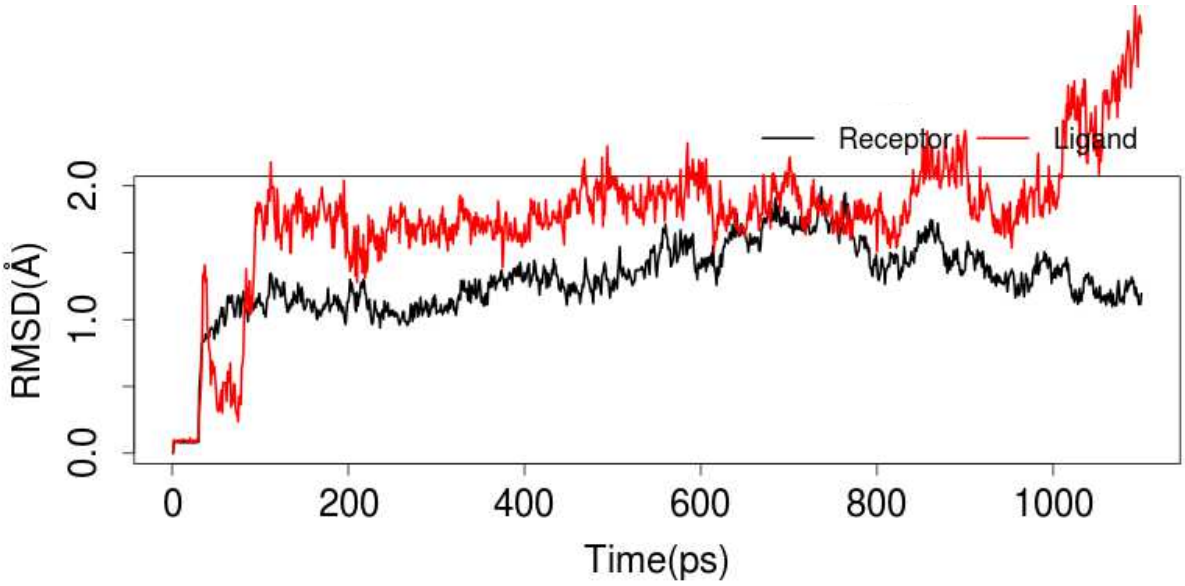

Fig 5b**:** The RMSD of the viral spike receptor and ligand

Receptor: Nucleocapsid Spike Glycoprotein; Ligand: Quercetin-3-o-rutinoside

The radius of gyration (Rg) was also considered to ascertain the changes in superimposed complex compactness. The radius of gyration measures the mass of atoms relative to the center of the mass of the complex. From the baseline trajectory, there was an increase in Rg starting from 200 ps simlution time, with an Rg complex of 14.3 nm, followed by sharp decrease of 13.9 nm, at 700 ps simulation. At 1000 ps, the Rg complex was 14.5 nm, which implies the compactness of the complex (Fig 6a). To further analyze the atomic postional fluctutaions of the residual RSMD, we considered the Root Mean Square Fluctuation (RMSF) of each residues. The fluctuation of each residue is calculated based on the CA atom of them. Residues at positions 30, 50 and 100 exhibited a higher fluctuation at 6Å, 6Å, and 8 Å respectively (Figure 6b).

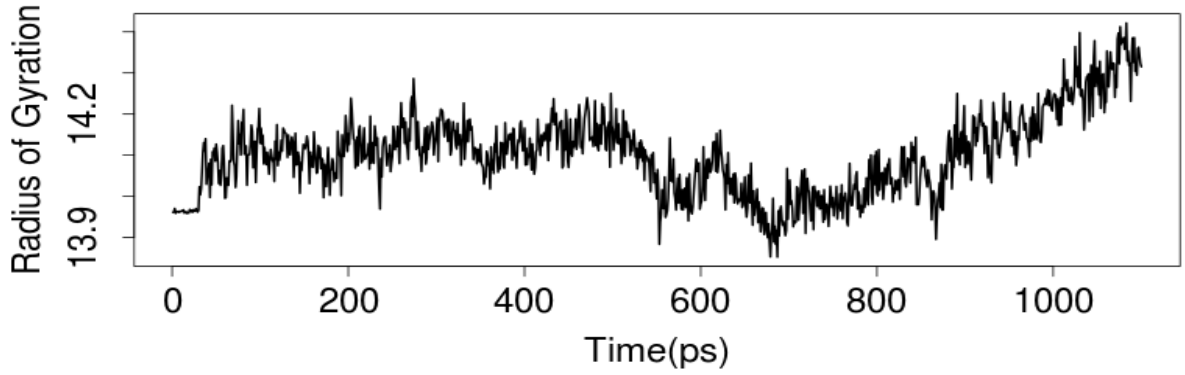

Fig 6a: The Radius of Gyration (Rg) plot of the docked complex

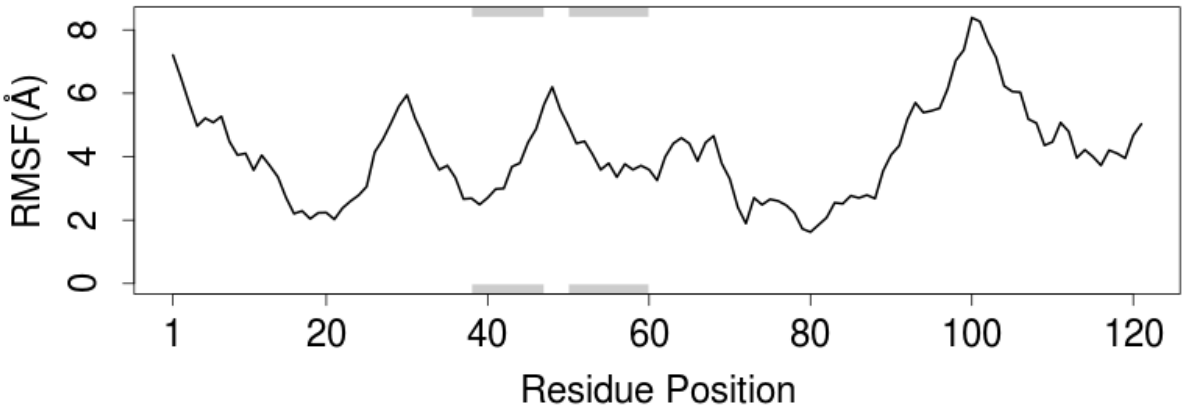

Fig. 6b: RMSF value of each residue. The secondary structure schematic is added to the top and bottom margins of figure (helices black, strands gray and loops white)

Residues cross correlation

The atomic fluctuations of the docked complex system are correlated with one another, which can be assessed by examining the magnitude of all pairwise cross-correlation coefficients. The residues with negative correlations are few in the complex (Figure 7)

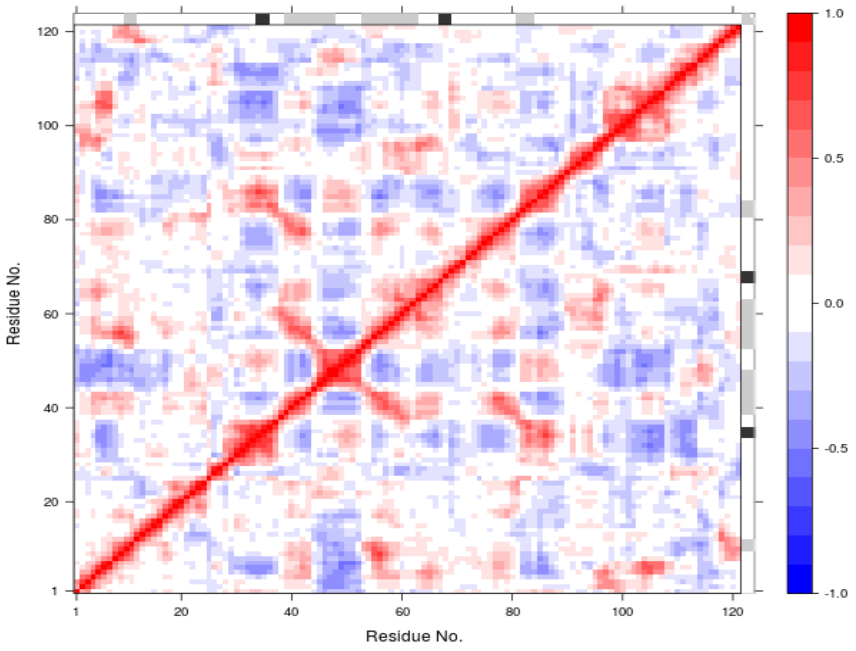

Fig 7: The cross residue correlation map of the atomic fluctuations of the spike receptor. The respective axis represents the residue indices on the Y axis and the decomposed parameters on the X axis. The secondary structure schematic is added to the top and right margins of dynamical residue cross-correlation map (helices black, strands gray and loops white).

Energy Calculations between the Ligand and the Protein receptor

The spike protein residues that contributes to the decompose results comprising of the electrostatic energy as calculated by the MM force field (TELE), van der Waals contribution from MM (TVDW), total gas phase energy (TGAS), sum of non-polar and polar contributions to solvation (TGBSOL), final estimated binding free energy calculated from the terms above (TGBTOT), are displayed in a heat map.The unit of them is kcal/mol (Fig. 8).

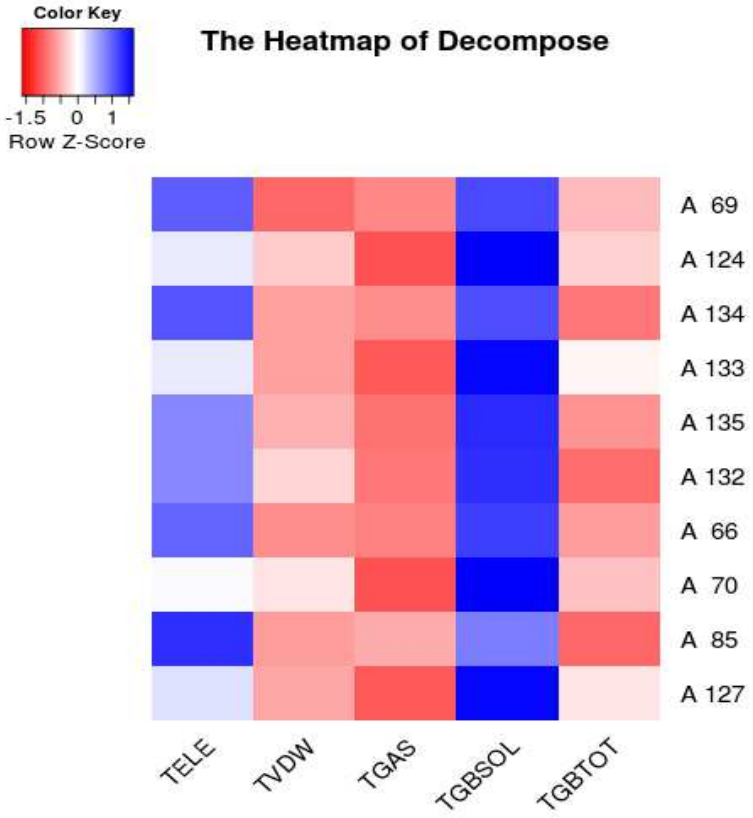

Fig. 8: The residues that contribute to various decompose calculations. The residues are ranked from top to bottom according to the energy ('TGBTOT'), and values are centered and scaled in the row direction shown with heat map.

Principal Cluster Analysis (PCA)

The PCA tool quantitatively evaluates the collective motion and measures the moment direction (Sarma et al., 2020; Pandey et al., 2020). The PCA and dynamic cross-correlation analysis were performed to evaluate the allosteric effect of SARS-CoV-2 spike protein under the ligand binding based on MD trajectory. This is to assess the direct and efficient mechanism for the modulation and regulation of cellular function in response to changes in concentration of small molecules. Therefore, 50% of the total variance of a given protein family structure can be captured by the principal components. This clearly provides a considerable insight on the nature of conformational differences. From the two clusters, the differential conformations can be studied. The value of both clusters is 27.1%. Hence, the PCA result of the spike protein and the ligand had no significant allostery (Fig. 9a and 9b).

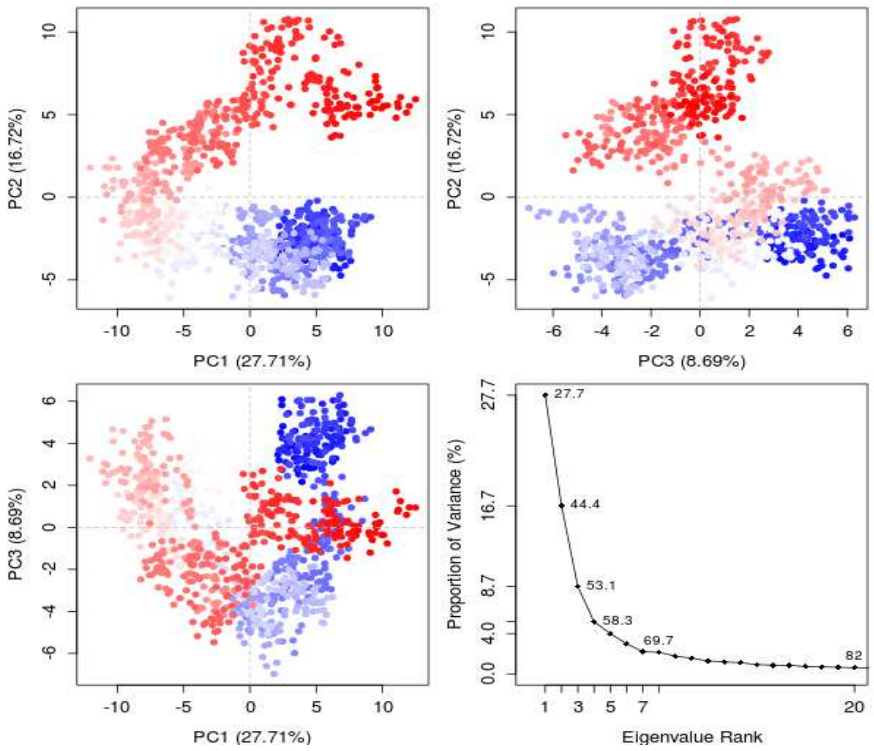

(9a)

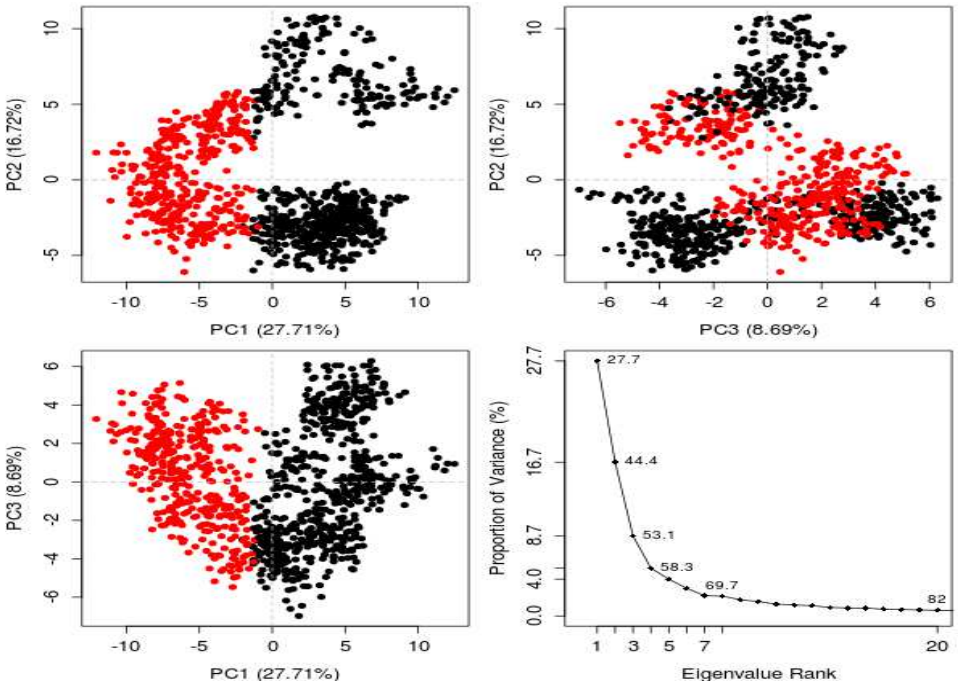

(9b)

Fig. 9a and 9b: The PCA cluster of conformations and residues cross correlation of the spike protein and ligand. The trajectory frames are highlighted in blue to white to red in time order. The N terminus is represented in blue, while the C-terminus is highlighted in red. The pink represents a pair of residues with correlation coefficient >0.8, and the blue lines depict a pair of residues with correlation coefficient <−0.4.

CONCLUSION

This work has identified quercetin-3-o-rutinoside as a direct inhibitor of SARS-CoV-2 spike protein through molecular docking analysis and prevents the interaction between human ACE-2 and SARS-CoV-2 spike protein which formed the key event of viral penetration and infection. The pharmacodynamics profile of quercetin-3-o-rutinoside depicted from the ADME toxicity reveal that, this compound is a safe therapeutic agent while the MD simulation predicted the stable bound or interaction of quercetin-3-o-rutinoside with the binding pocket of SARS-CoV-2 spike protein.

Ethical statement

The study does not involve the animals.

Declaration of competing interest

The authors declare no competing interests.

Data availability

The 3D and 2D docking structures are available upon request from the corresponding author.

References

1. Masters, P.S. (2006). The molecular biology of coronaviruses. Adv. Virus Res. 66: 193–292.
2. Rahman, N., Basharat, Z., Yousuf, M., Castaldo, G., Rastrelli, L., & Khan. H. (2020). Virtual Screening of Natural Products against Type II Transmembrane Serine Protease (TMPRSS2), the Priming Agent of Coronavirus 2 (SARS-CoV-2). Molecules. 25: 2271; doi:10.3390/molecules25102271
3. Kadioglu, O., Saeed, M., Johannes, G. H., & Efferth, T. (2020) Identification of novel compounds against three targets of SARS CoV-2 coronavirus by combined virtual screening and supervised machine learning. Bull World Health Organ. Preprint.
4. Omotuyi, I. O., Nash, O., Ajiboye, B. O., Metibemu, D. S., Oyinloye, B. E., Adelakun, N. S., Hurdayal, R., Aruleba R. T., & Kappo, A. P. (2020). Darunavir Disrupts Critical Nodes in Metastable 2019-nCoV-RBD/ACE-2 Complex. Preprint doi:10.20944/preprints202003.0125.v1
5. Madjid, M., Safavi-Naeini, P., Solomon, S. D., & Vardeny, O. (2020). Potential Effects of Coronaviruses on the Cardiovascular System: A Review. JAMA Cardiol. doi: 10.1001/jamacardio.2020.1286.
6. Zhang, Y., Zheng, N., Haoc, P., Caod, Y. & Zhonga, Y. (2005). A molecular docking model of SARS-CoV S1 protein in complex with its receptor, human ACE2. Computational Biology and Chemistry. 29: 254–257. doi:10.1016/j.compbiolchem.2005.04.008
7. Pandey, P., Rane, J. S., Chatterjee, A., Kumar, A., Khan, R., Prakash, A., & Ray, S. (2020) Targeting SARS-CoV-2 spike protein of COVID-19 with naturally occurring phytochemicals: an in silico study for drug development. Journal of Biomolecular Structure and Dynamics https://doi.org/10.1080/07391102.2020.1796811.
8. Hoffmann, M., Kleine-Weber, H., Schroeder, S., Kruger, N., Herrler, T., & Erichsen, S. (2020). SARS-CoV-2 Cell Entry Depends on ACE2 and TMPRSS2 and Is Blocked by a Clinically Proven Protease Inhibitor. Cell. 181(2):271. doi: 10.1016/j.cell.2020.02.052.

9. Patel, D., Chirag, N. S., Prasanth, K., Pandya, D., Himanshu. A., Rawal, D., & Rakesh, M. (2020): Identification of Potential Binders of the SARS-Cov-2 Spike Protein via Molecular Docking, Dynamics Simulation and Binding Free Energy Calculation. ChemRxiv. Preprint. https://doi.org/10.26434/chemrxiv.12278588.v1
10. Zhang, D., Wu, K., Zhang, X., Deng, S., & Peng, B. (2020). In silico screening of Chinese herbal medicines with the potential to directly inhibit 2019 novel coronavirus. Journal of Integrative Medicine 18 (2020) 152–158
11. Chen, G., Yao, T., Ahmed, A., Pan, Y., Yang, J., & Wu, Y. (2020). The discovery of potential natural products for targeting SARS-CoV-2 spike protein by virtual screening. BioRxiv. preprint doi: https://doi.org/10.1101/2020.06.25.170639
12. Biancatelli, R. M. L., Berrill, M., Catravas, J. D., & Marik, P. E. (2020). Quercetin and Vitamin C: An Experimental, Synergistic Therapy for the Prevention and Treatment of SARS-CoV-2 Related Disease (COVID-19). Front. Immunol. 11:1451. doi: 10.3389/fimmu.2020.01451
13. Robaszkiewicz, A., Balcerczyk, A., & Bartosz, G. (2007). Antioxidative and prooxidative effects of quercetin on A549 cells. Cell Biol Int. 31: 1245– 50. doi: 10.1016/j.cellbi.2007.04.009
14. Nair, M. P., Kandaswami, C., Mahajan, S., Chadha, K. C., Chawda, R., & Nair, H. (2002). The flavonoid, quercetin, differentially regulates Th-1 (IFN_) and Th-2 (IL4) cytokine gene expression by normal peripheral blood mononuclear cells. Biochim Biophys Acta. 1593:29–36.
15. Uchide, N., & Toyoda, H. (2011). Antioxidant therapy as a potential approach to severe influenza-associated complications. Molecules. 16: 2032–52. doi:10.3390/molecules16032032
16. Balogun, T. A., Omoboyowa, D. A. & Saibu, O. A. (2020). *In silico* Anti-malaria Activity of Quinolone Compounds against *Plasmodium falciparum* Dihydrofolate Reductase (pfDHFR). *International Journal of Biochemistry Research & Review. 29(8): 10-17, 2020.* DOI: 10.9734/IJBCRR/2020/v29i830208
17. Cheng, F., Li, W., Zhou, Y., Shen, J., Wu, Z., Liu, G., Lee, P. W., & Tang, Y. (2012) admetSAR: a comprehensive source and free tool for evaluating chemical ADMET properties, J. Chem. Inf. Model. *52(11)*: 3099–3105

doi:http://dx.doi.org/10.2471/BLT.20.255943

18. Maier, J. A., Martinez, C., & Kasavajhala, K. (2015). ff14SB: improving the accuracy of protein side chain and backbone parameters from ff99SB. J Chem Theory Comput. *11*: 3696 – 3713.
19. Wang, J., Wolf, R. M., Caldwell, J. W., & Kollman, P. A. (2004). Development and testing of a general amber force field. Case DAJ Comput Chem. *25(9)*: 1157 - 1174.
20. Horn, H. W., Swope, W. C., Pitera, J. W., Madura, J. D., Dick, T. J., Hura, G. L., & Head-Gordon, T. J. (2004). Development of an improved four-site water model for biomolecular simulations: TIP4P-Ew. Chem Phys. *120(20)*: 9665-9667
21. McGibbon, R. T., Beauchamp, K. A., & Harrigan, M. P. (2015). MDTraj: a modern open library for the analysis of molecular dynamics trajectories. Biophys J. *109*: 1528 – 1532
22. Grant, B. J., Rodrigues, A. P., & ElSawy, K. M. (2006). Bio3d: an R package for the comparative analysis of protein structures. Bioinformatics. *22*: 2695–2696.
23. Heinz, S. A., Henson, D. A., Austin, M. D., Jin, F., & Nieman, D. C. Quercetin supplementation and upper respiratory tract infection: A randomized community clinical trial. Pharmacological Research 62 (2010) 237–242
24. Veber, D. F., Johnson, S. R., Cheng, H. Y., Smith, B. R., Ward, K. W. & Kopple, K. D. (2002). Molecular properties that influence theoral bioavaliability of drug candidate, J. Med. Chem. 5(12): 2615–2623.
25. Yan, A., Wang, Z., & Cai, Z. (2008). Prediction of human intestinal absorption by GA feature selection and support vector machine regression, Int. J. Mol. Sci. 9(10): 1961–1976, doi:10.3390/ijms9101961.
26. Ballabh, P., Braun, A., & Nedergaard, M. (2004). The blood–brain barrier: an overview: structure, regulation, and clinical implications, Neurobiol. Dis. 16: 1–13.
27. Zhou, S. (2008). Drugs Behave as Substrates, Inhibitors and Inducers of Human Cytochrome P450 3A4, Curr. Drug Metab. 9: 310, doi:10.2174/138920008784220664.
28. Sarma, P., Shekhar, N., Prajapat, M., Avti, P., Kaur, H., Kumar, S., Singh, S., Kumar, H., Prakash, A., Dhibar, D. P., & Medhi, B. (2020). In-silico homology assisted identification of inhibitor of RNA binding against 2019- nCoV N-protein (N terminal domain). Journal of Biomolecular Structure and Dynamics, 1–9. https://doi.org/10.1080/07391102.2020.1753580

Figures

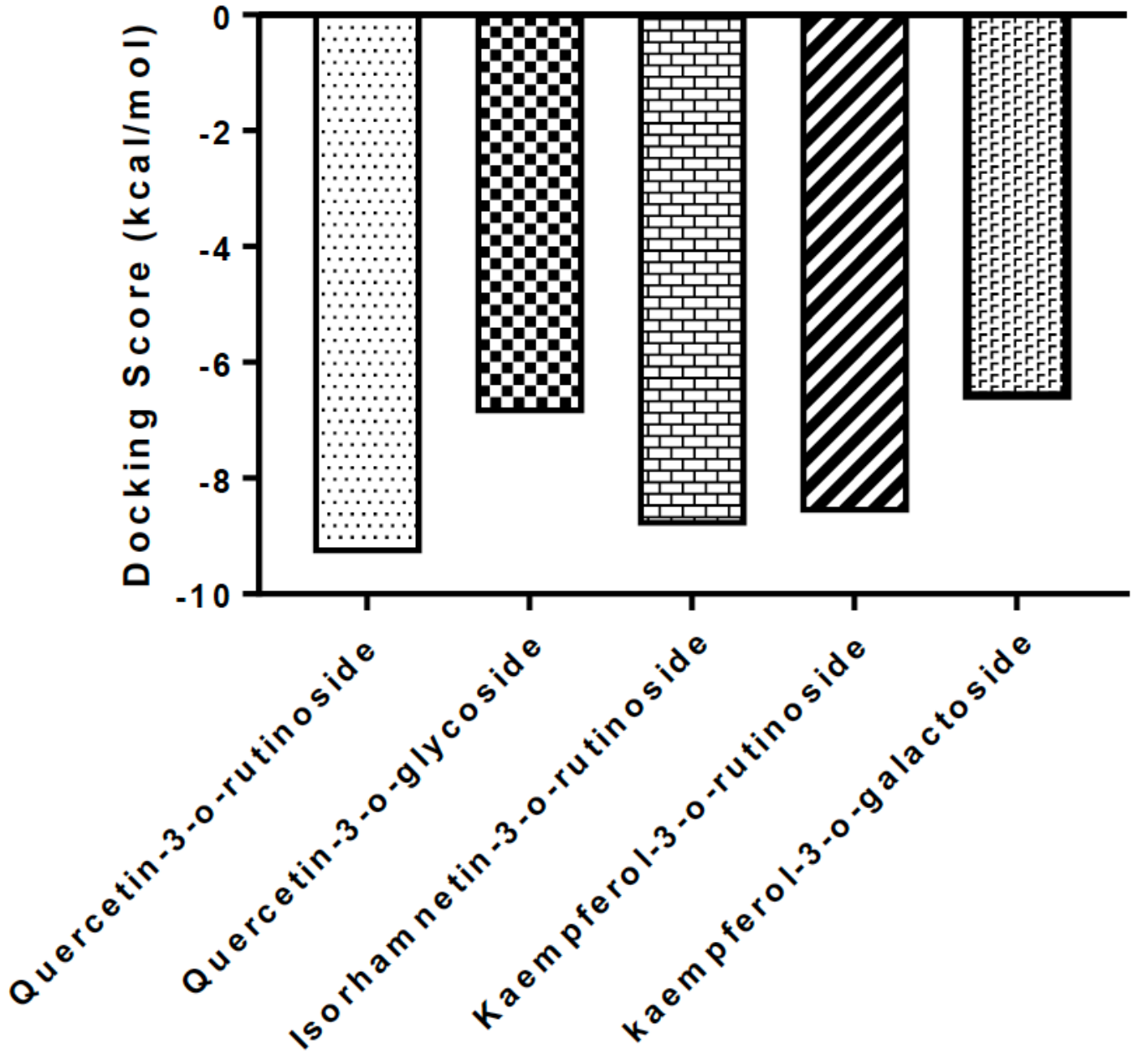

Figure 1

The binding affinity (kcal/mol) for the docking of the natural compounds against Nucleocapsid Spike Glycoprotein

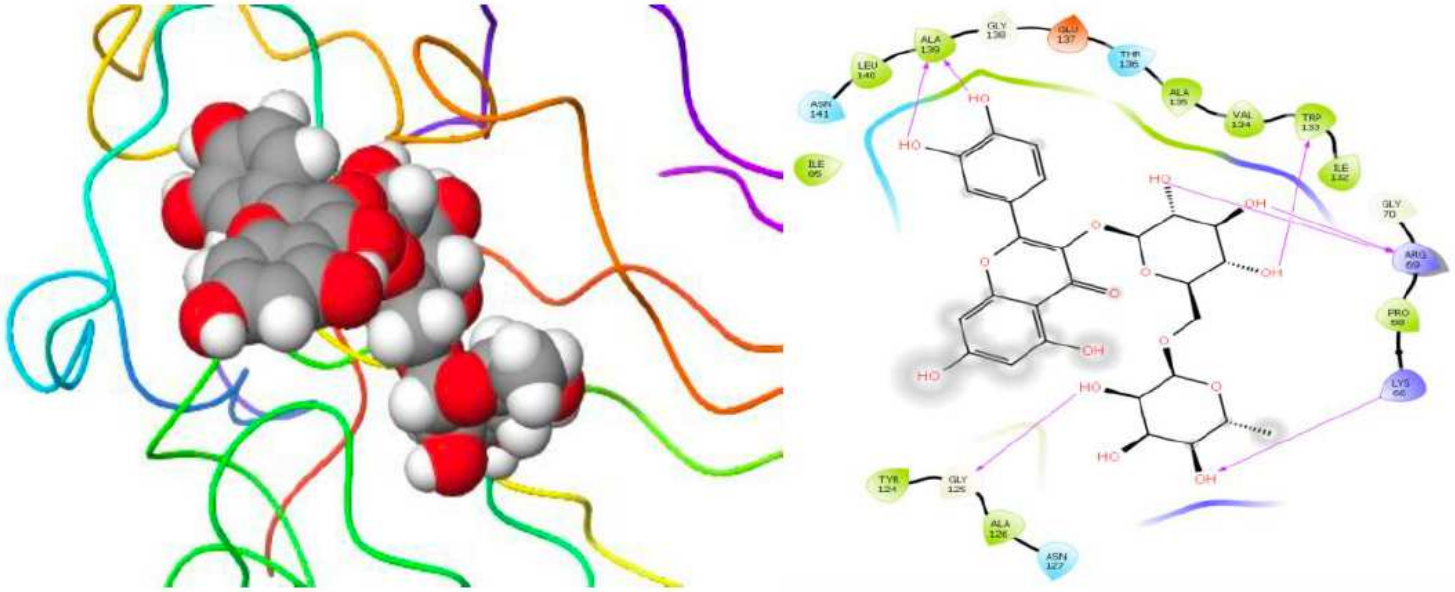

Figure 2

Protein-ligand interaction of quercetin-3-o-rutinoside against spike glycoprotein

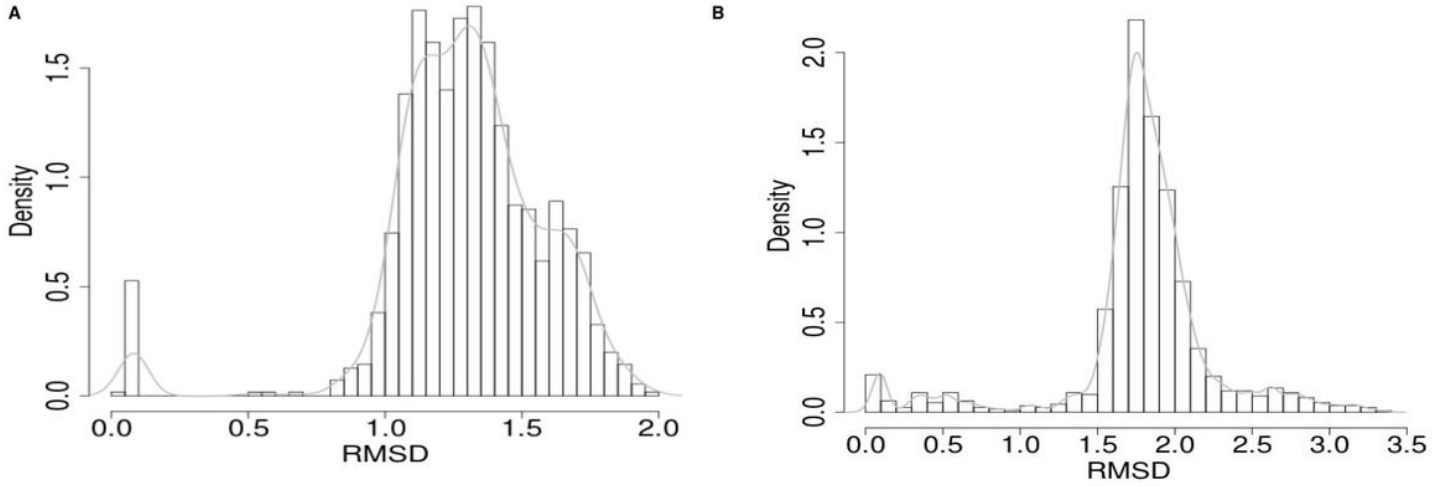

Figure 3

A. Generated RSMD histogram of the spike receptor. B. Generated RSMD plot for the ligand

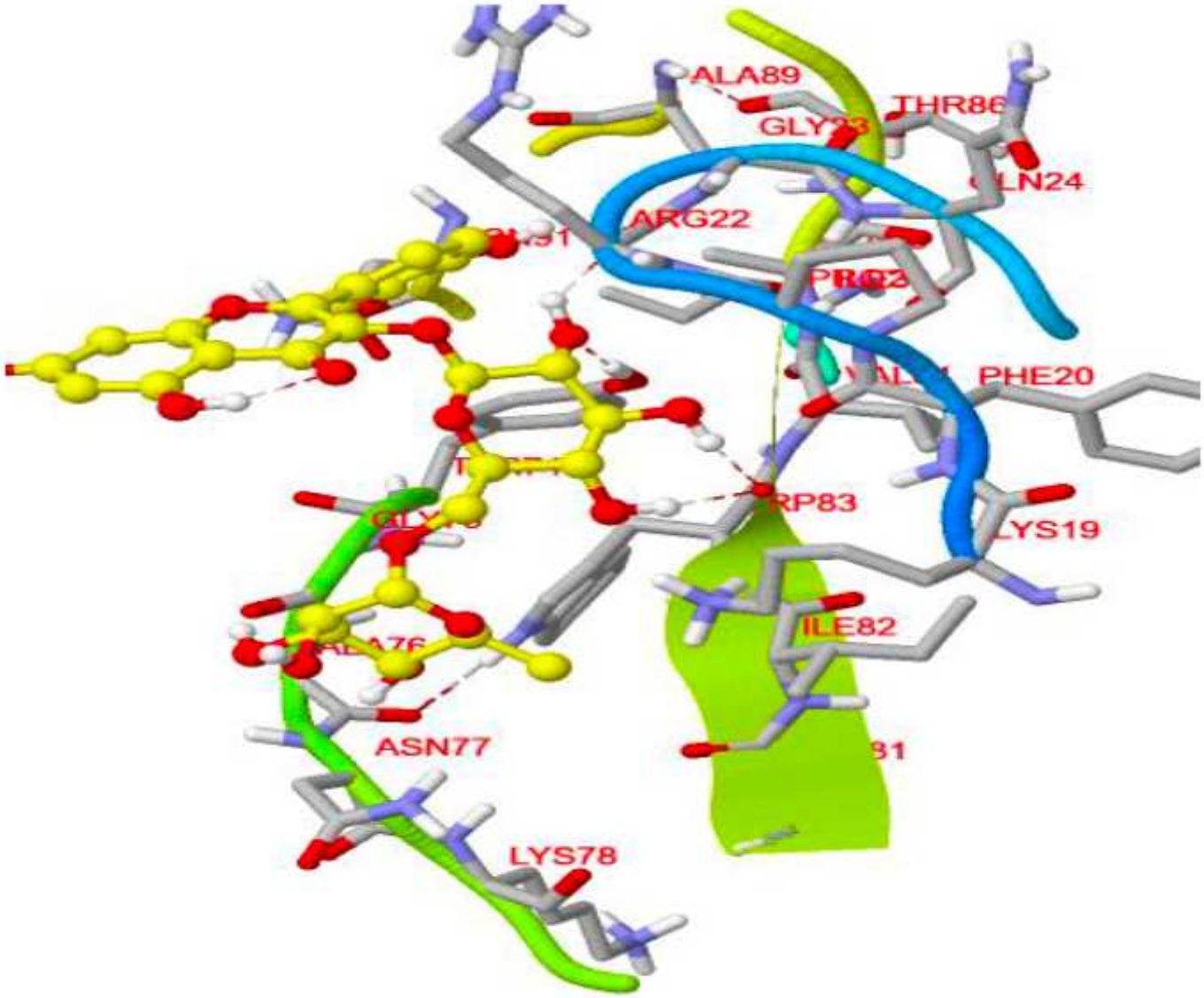

Figure 4

Native contacts between Spike protein residues and quercetin-3-o-rutinoside complex.

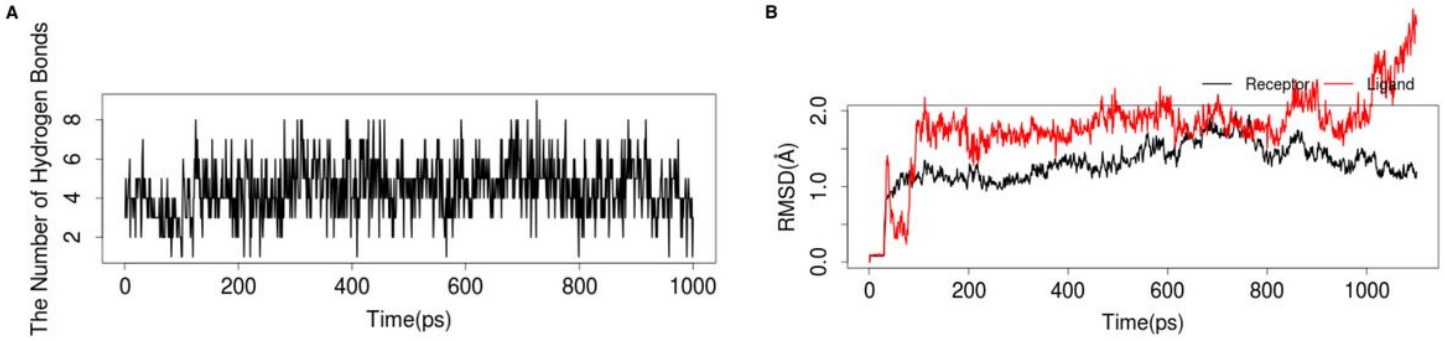

Figure 5

A. The number of hydrogen interactions between the ligand and the protein. B. The RMSD of the viral spike receptor and ligand Receptor: Nucleocapsid Spike Glycoprotein; Ligand: Quercetin-3-o-rutinoside

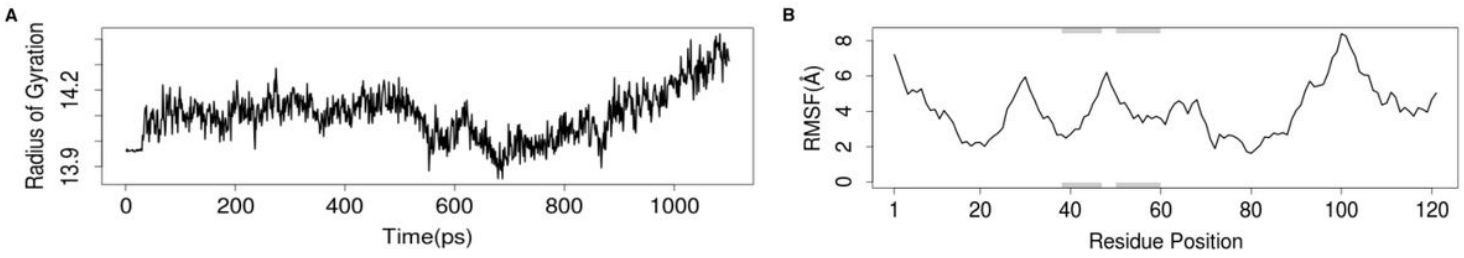

Figure 6

A. The Radius of Gyration (Rg) plot of the docked complex. B. RMSF value of each residue. The secondary structure schematic is added to the top and bottom margins of figure (helices black, strands gray and loops white)

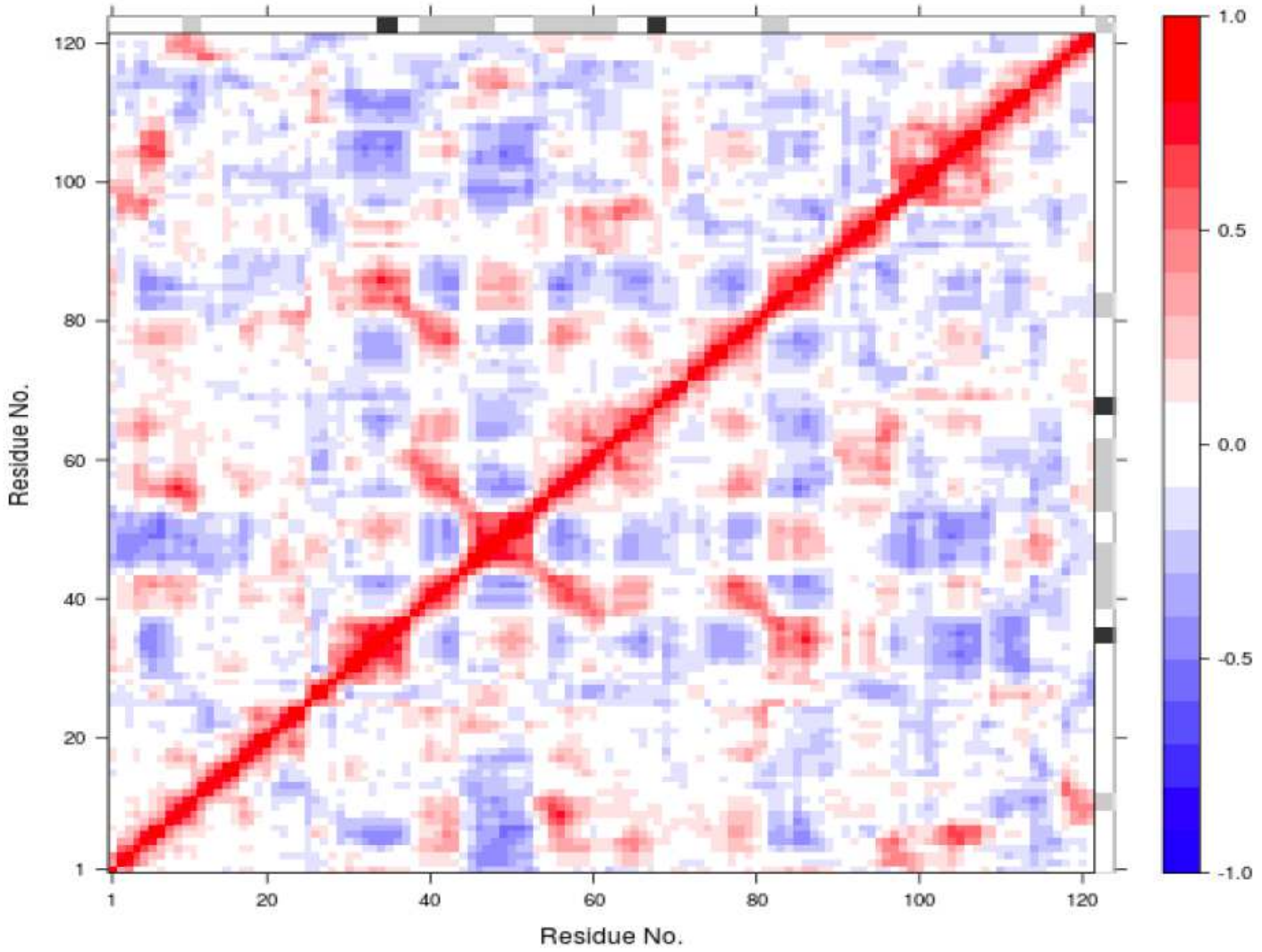

Figure 7

The cross residue correlation map of the atomic fluctuations of the spike receptor. The respective axis represents the residue indices on the Y axis and the decomposed parameters on the X axis. The secondary structure schematic is added to the top and right margins of dynamical residue cross-correlation map (helices black, strands gray and loops white).

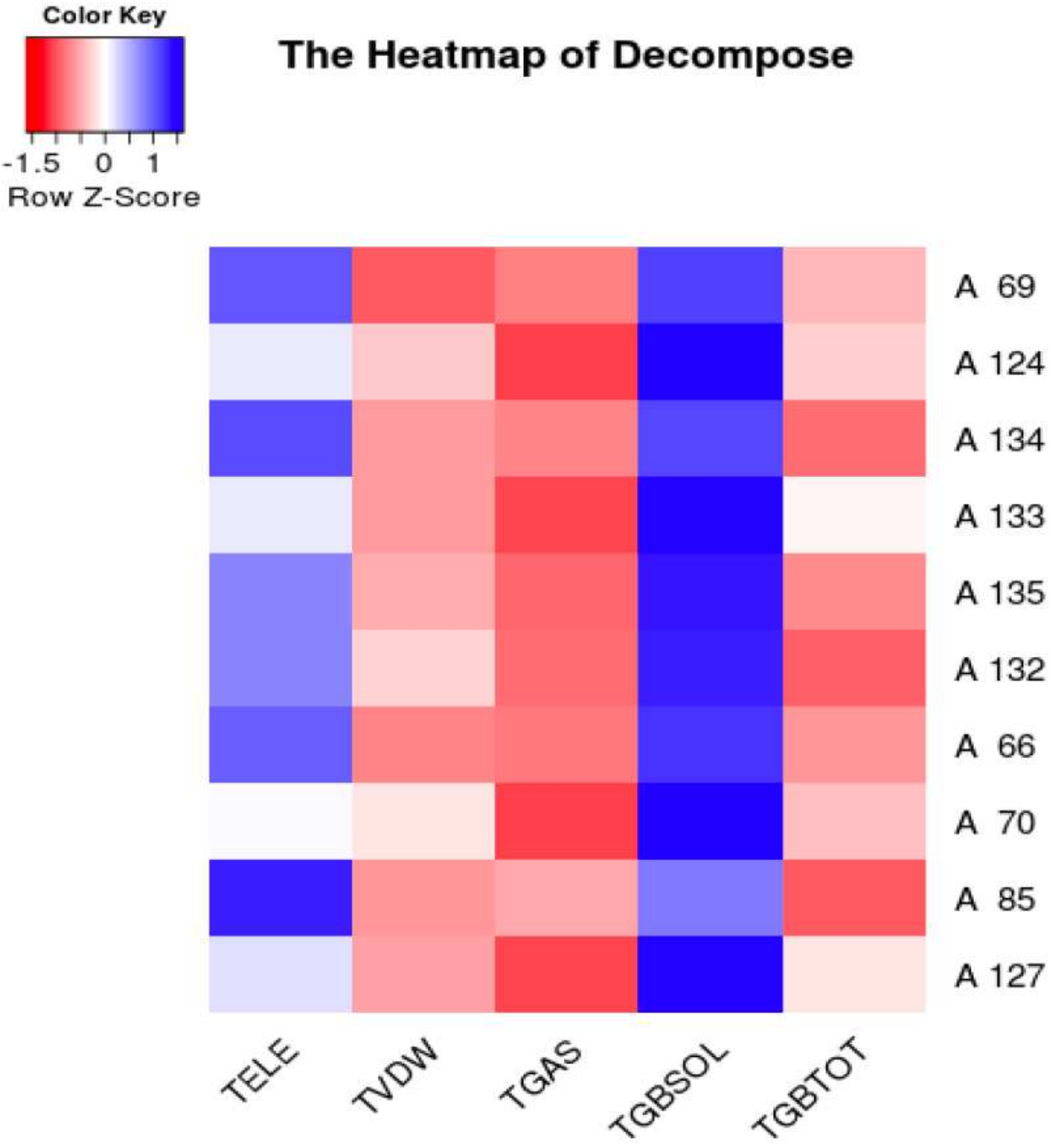

Figure 8

The residues that contribute to various decompose calculations. The residues are ranked from top to bottom according to the energy ('TGBTOT'), and values are centered and scaled in the row direction shown with heat map.

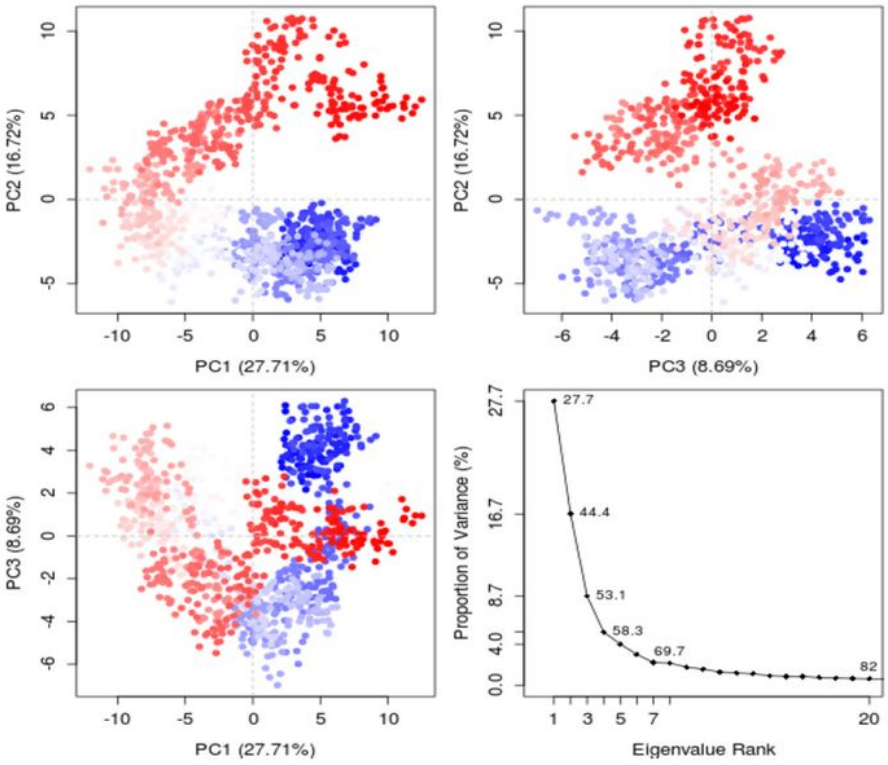

(9a)

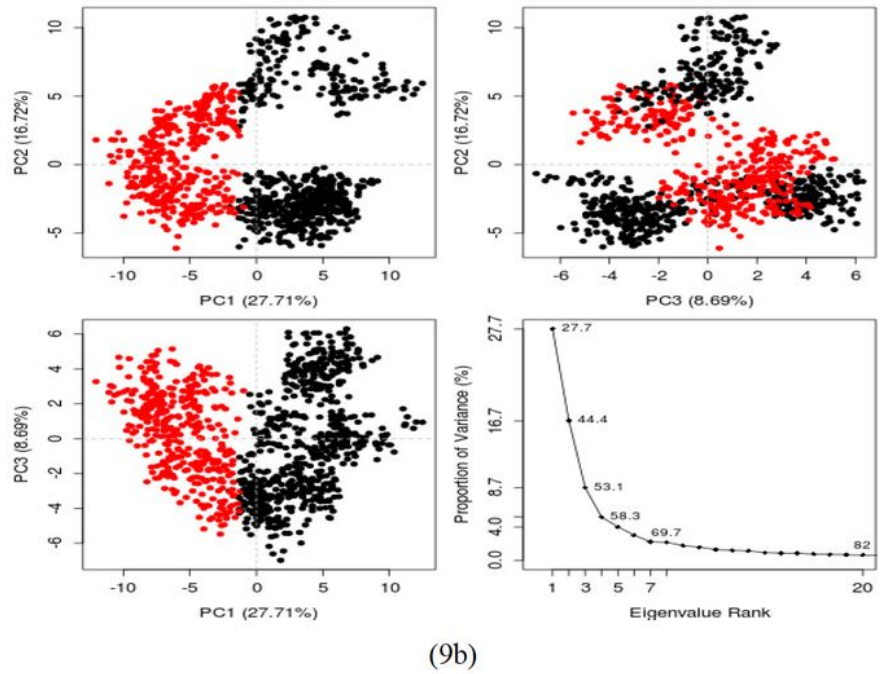

(9b)

Figure 9

A and B: The PCA cluster of conformations and residues cross correlation of the spike protein and ligand. The trajectory frames are highlighted in blue to white to red in time order. The N terminus is represented in

blue, while the C-terminus is highlighted in red. The pink represents a pair of residues with correlation coefficient >0.8, and the blue lines depict a pair of residues with correlation coefficient <−0.4.